



# Charge-density-wave superconductor Bi<sub>2</sub>Rh<sub>3</sub>Se<sub>2</sub>

著者	Sakamoto Takeshi, Wakeshima Makoto, Hinatsu Yukio, Matsuhira Kazuyuki
journal or publication title	Physical Review B
volume	75
number	060503
page range	060503-1-060503-4
year	2007
URL	<a href="http://hdl.handle.net/10228/637">http://hdl.handle.net/10228/637</a>

doi: 10.1103/PhysRevB.75.060503

## Charge-density-wave superconductor $\text{Bi}_2\text{Rh}_3\text{Se}_2$

Takeshi Sakamoto, Makoto Wakeshima,\* and Yukio Hinatsu

*Division of Chemistry, Graduate School of Science, Hokkaido University, Sapporo 060-0810, Japan*

Kazuyuki Matsuhira

*Department of Electronics, Faculty of Engineering, Kyushu Institute of Technology, Kitakyushu 804-8550, Japan*

(Received 12 January 2007; published 16 February 2007)

We discovered a superconducting transition with the charge-density-wave state in a ternary compound  $\text{Bi}_2\text{Rh}_3\text{Se}_2$ . This compound crystallizes in the parkerite-type structure composed of sheets containing one-dimensional Rh-Rh chains. The electrical resistivity, magnetic susceptibility, thermoelectric power, sample length change, and x-ray diffraction measurements reveal that this compound is in the CDW state below 240 K. Furthermore, the specific heat and electrical resistivity measurements show a superconducting transition at  $\sim 0.7$  K. The various superconducting parameters were determined, and the GL parameter  $\kappa(0)$  shows the considerably large value of 151 indicating an extreme type-II superconductor.

DOI: [10.1103/PhysRevB.75.060503](https://doi.org/10.1103/PhysRevB.75.060503)

PACS number(s): 74.70.Dd, 72.15.Eb, 74.25.Fy

Collective states showing exotic electronic properties, such as superconductivity and charge-density-wave (CDW), have attracted a lot of interest. Peierls pointed out in his book that an electron-phonon interaction resulted in periodic and dielectric lattice distortions with a phase transition from metallic to insulating conductivity.<sup>1</sup> At the same time, Fröhlich suggested a sliding of the collective state involving lattice displacements and electrons in the one-dimensional metal as a mechanism of superconductivity.<sup>2</sup> His concept had been forgotten by an appearance of the Bardeen-Cooper-Schrieffer (BCS) theory but has revived in researches on the CDW state in one-dimensional conductors. The CDW state with such lattice distortions competes with a superconducting state because of the dielectric gapping of Fermi surface.

Recently, Gabovich and co-workers reviewed the properties of superconductors with CDW and discussed the competition between the CDW and superconducting states.<sup>3,4</sup> Most of the CDW superconductivities were found in compounds with the well-known crystal structures; i.e., layered chalcogenides, NbSe<sub>3</sub>, A15-, and C15-type intermetallic compounds, and so on. In these compounds, partial dielectric gapping causes a detrimental effect on superconductivity.

In this study, we have synthesized successfully a novel ternary compound  $\text{Bi}_2\text{Rh}_3\text{Se}_2$  and have investigated its crystal structure and transport properties. This compound is found to crystallize in a parkerite-type structure<sup>5</sup> composed of sheets containing one-dimensional Rh-Rh chains. As in metal-rich chalcogenides, a superconducting transition with the CDW state was first discovered through the electrical resistivity, magnetic susceptibility, specific heat, thermoelectric power, sample length change, and x-ray diffraction measurements.

A polycrystalline  $\text{Bi}_2\text{Rh}_3\text{Se}_2$  was prepared by mixing Bi, Rh, and Se in the stoichiometric ratio and heating in a silica tube at 1320 K for 6 h. It was cooled slowly (2 K/h) to 1020 K, and then quenched. Unfortunately, we could not obtain products for a single crystal structure analysis because of formation of twin or much more crystals. Thus, the crystal structure of the obtained product was identified by powder x-ray diffraction measurements (Rigaku

RINT 2000 diffractometer) between 30 and 300 K.

Magnetic susceptibilities were measured from 1.8 to 400 K in an applied field of 1 T using a superconducting quantum interference device magnetometer (Quantum Design, MPMS-5S). Electrical resistivity measurements were carried out in the temperature range of 0.35–400 K and in magnetic fields up to 1.5 T by a four-probe method in a Quantum Design PPMS equipped with a <sup>3</sup>He refrigerator. Specific heat measurement was performed from 0.35 to 300 K by the thermal relaxation method with the PPMS. The thermoelectric power (TEP) was measured in the temperature range between 10 and 300 K by a differential method. The sample length change was measured by using strain gauges from 5 to 300 K. The copper expansivities were used to convert the experimental relative length changes to the absolute values.

The x-ray diffraction measurement at room temperature reveals that the obtained product crystallizes in a parkerite-type structure as a single phase. By the Rietveld analysis using RIETAN2000,<sup>6</sup> the lattice parameters were determined to be  $a=11.414(10)$  Å,  $b=8.3709(9)$  Å,  $c=11.989(1)$  Å,  $\beta=89.153(3)^\circ$  (reliable factors;  $R_{\text{wp}}=12.9\%$ ,  $R_I=4.2\%$ ).

The schematic crystal structure of  $\text{Bi}_2\text{Rh}_3\text{Se}_2$  is illustrated in Fig. 1. In this structure, rhodium atoms are coordinated by selenium [ $d(\text{Rh}-\text{Se})=2.39\text{--}2.41$  Å], bismuth [ $d(\text{Rh}-\text{Bi})=2.70\text{--}2.93$  Å], and Rh [ $d(\text{Rh}-\text{Rh})=2.86\text{--}2.99$  Å]. The Rh-Rh bondings form one-dimensional chains along the  $a$ -axis having the short interatomic distances of  $d(\text{Rh1}-\text{Rh4})=2.86$  Å and  $d(\text{Rh2}-\text{Rh3})=2.86$  Å. These Rh chains are connected by Rh6 and Rh5 atoms with the longer Rh-Rh distances [ $d(\text{Rh1}-\text{Rh6})=2.99$  Å and  $d(\text{Rh2}-\text{Rh5})=2.87$  Å], forming two-dimensional sheets perpendicular to the  $c$  axis. The shortest interatomic distance between two-dimensional sheets is 3.25 Å for the Bi-Se bonding, and this feature of the pseudo-two-dimensional crystal structure will cause low-dimensional peculiar behavior.

Figure 2(a) shows the temperature dependence of the electrical resistivity  $\rho$ . A superconducting transition is observed at 0.9 K, as will be discussed later. Above 260 K, the resistivity increases linearly with temperature, indicating a

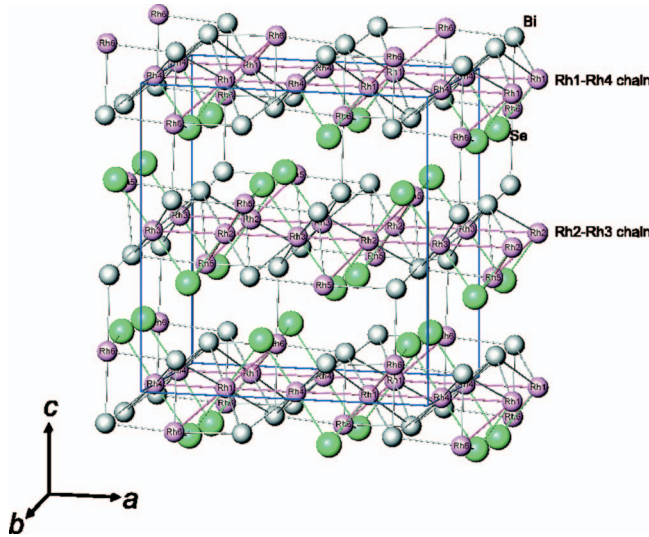


FIG. 1. (Color) Schematic crystal structure of  $\text{Bi}_2\text{Rh}_3\text{Se}_2$ .

typical metallic behavior. Below 250 K, the resistivity increases gradually with decreasing temperature and has a maximum around 190 K. Below 190 K, the resistivity shows a metallic behavior down to 1 K again. No hysteresis in the resistivity between the cooling and heating processes was observed around the anomaly temperature ( $\sim 250$  K), indicating that this phase transition is the second-order one.

Figure 2(b) shows the temperature dependence of the magnetic susceptibility  $\chi$  after a diamagnetic correction ( $\chi_{\text{dia}} = 2.66 \times 10^{-4}$  emu mol $^{-1}$ ). The positive values of  $\chi$  indicate that Pauli paramagnetism dominates the magnetic susceptibilities in this compound. A Curie paramagnetic behavior at low temperatures is attributable to a small amount ( $< 1.5\%$ ) of paramagnetic impurities which is undetectable in the x-ray diffraction profile. With decreasing temperature below 250 K,  $\chi$  drops. The Pauli paramagnetic and Landau

diamagnetic susceptibilities can be represented by  $\chi_{\text{Pauli}} + \chi_{\text{Landau}} = N_A \mu_0 \mu_B^2 [1 - m^2/3m^*] N(\epsilon_F) \propto N(\epsilon_F)$  using the density of states at the Fermi level  $N(\epsilon_F)$ . The drop of  $\chi$ , which corresponds to the raise of  $\rho$ , indicates a loss of conduction electrons.

The temperature dependence of the thermoelectric power TEP for  $\text{Bi}_2\text{Rh}_3\text{Se}_2$  is shown in Fig. 2(c). The TEP is negative over the whole temperature range. The value of TEP increases linearly with decreasing temperature and reaches a maximum at  $\sim 250$  K. Below this temperature, TEP decreases rapidly, followed by a minimum at 95 K. Furthermore, with decreasing temperature, TEP increases toward zero and has a shoulder around 30 K ( $\sim \Theta_D/6$ ;  $\Theta_D$  is the Debye temperature) due to a phonon-drag, indicating a typical metallic behavior. The maximum at  $\sim 250$  K is consistent with the onset of the anomaly as shown in the  $\rho$ - $T$  and  $\chi$ - $T$  curves. Since the TEP measurement is a sensitive probe of the density of states close to the Fermi surface, the rapid change around 250 K is attributable to the sudden change of the band structure.

Figure 2(d) shows the temperature dependence of the sample length change  $\epsilon (= \delta L/L)$ . A shoulder is observed around 240 K in the  $\epsilon$ - $T$  curve. To clarify this anomaly, the first derivative of  $\epsilon$  is also plotted in the same figure. A sharp peak is found at 242 K, indicating a lattice transformation in the  $\text{Bi}_2\text{Rh}_3\text{Se}_2$ . As observed in the  $T$  dependence of  $\rho$ ,  $\chi$ , TEP, and  $\epsilon$ , it is considered that the second-order phase transition at  $\sim 250$  K is caused by a deformation of the Fermi surface. Similar transitions are found in some CDW compounds.<sup>3,4,7</sup>

In order to clarify the anomaly at  $\sim 250$  K due to the CDW transition, we have carried out the x-ray diffraction measurements below 300 K. Figure 3(a) shows the x-ray diffraction profiles at 100 and 300 K in which the logarithm value of intensity is plotted as the longitudinal axis. In the  $2\theta$  range between  $10^\circ$  and  $40^\circ$ , only one additional diffraction peak is found at  $\sim 35.5^\circ$ . It is difficult to index this peak because of its broadness due to the overlap with some other reflections in this  $2\theta$  region. This superlattice peak at several temperatures is normalized [see Fig. 3(b)] and the integrated peak intensity is plotted as a function of temperature in Fig. 3(c). The superlattice reflection for a CDW phase gives directly the CDW gap  $\Delta_{\text{CDW}}$ , i.e., the intensity is proportional to  $\Delta_{\text{CDW}}^2$ .<sup>7</sup> According to the mean-field BCS theory,  $\Delta_{\text{CDW}}$  can be represented by  $\Delta_{\text{CDW}}(T)/\Delta_{\text{CDW}}(0) = \tanh\{(T_{\text{CDW}}/T) \times [\Delta_{\text{CDW}}(T)/\Delta_{\text{CDW}}(0)]\}$ . The normalized  $\Delta_{\text{CDW}}^2$  is also plotted as a solid line in Fig. 3(c) and is in good agreement with the obtained superlattice intensities. This behavior is consistent with that for the CDW compounds  $\text{NbSe}_3$ ,  $(\text{TaSe}_4)_2\text{I}$  and  $\text{K}_{0.3}\text{MoO}_3$ . Unfortunately, we could not determine a wave vector of the CDW state from the powder x-ray diffraction. However, based on the results of the  $\rho$ ,  $\chi$ , TEP,  $\epsilon$ , and low-temperature x-ray measurements, we can conclude that the anomaly at  $\sim 250$  K is the second-order phase transition from the normal metallic state to the CDW state with metallic conductivity.

Figures 4(a) and 4(b) shows the temperature and field dependences of resistivity of  $\text{Bi}_2\text{Rh}_3\text{Se}_2$ , respectively. As shown in Fig. 4(a), the resistivity in the zero field drops

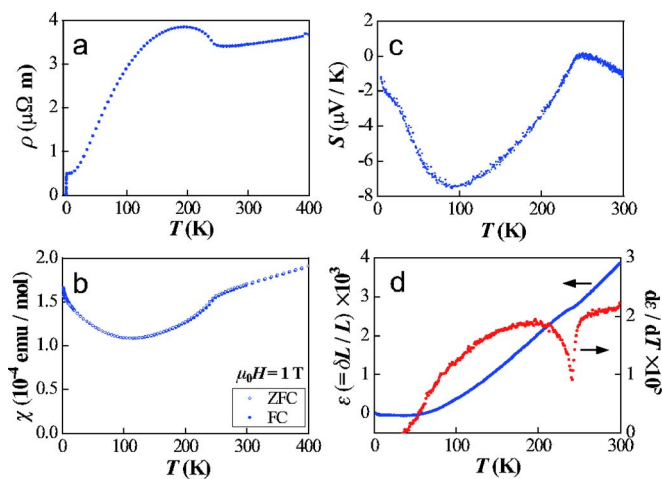


FIG. 2. (Color online) (a) Temperature dependence of the electrical resistivity ( $\rho$ ). (b) Temperature dependence of the magnetic susceptibility ( $\chi$ ) in a magnetic field  $\mu_0 H = 1$  T. (c) Temperature dependence of the thermoelectric power ( $S$ ). (d) Temperature dependence of the sample length change ( $\epsilon$ ) and its first derivative ( $d\epsilon/dT$ ).

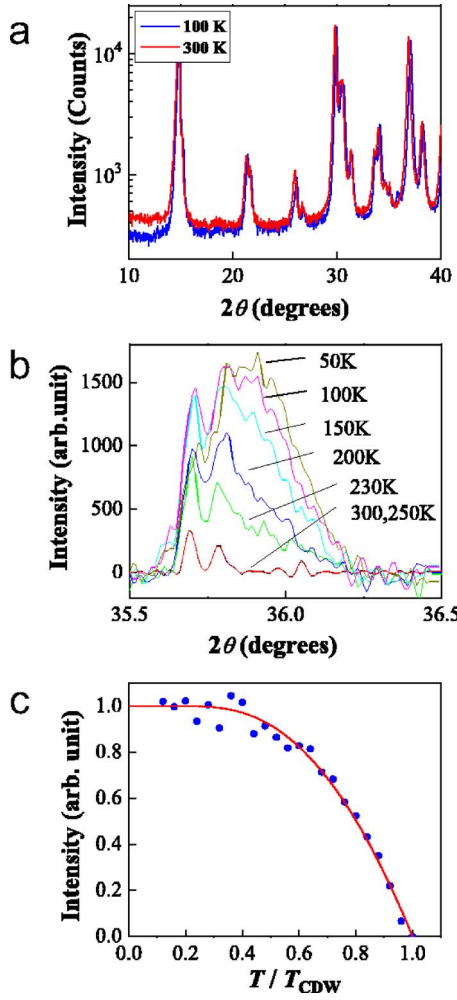


FIG. 3. (Color online) (a) Powder x-ray diffraction profiles at 100 and 300 K. (b) Powder x-ray diffraction profiles in the  $2\theta$  range between  $35.5^\circ$  and  $36.5^\circ$  at several temperatures. (c) Temperature dependence of the normalized superlattice integrated intensity.

abruptly below 0.92 K with decreasing temperature, indicating a phase transition to a superconducting state. The zero resistivity is attained below 0.76 K. The critical temperature  $T_c$  is defined as the midpoint of the transition  $T_c^{\text{mid},R} = 0.84$  K.

The value of  $T_c^{\text{mid},R}$  decreases with increasing applied field [see Fig. 4(a)]. Assuming that  $\text{Bi}_2\text{Rh}_3\text{Se}_2$  is a type-II superconductor, as will be justified below, the upper critical field  $\mu_0 H_{c2}(T)$  was determined from Figs. 4(a) and 4(b). Figure 4(c) shows  $\mu_0 H_{c2}(T)$  as a function of the critical temperature. According to the Werthamer-Helfand-Hohenberg (WHH) theory for a type-II superconductor in the dirty limit,<sup>8</sup> the upper critical field at zero temperature can be estimated from the relation  $\mu_0 H_{c2}(0) = 0.693 T_c [-d\mu_0 H_{c2}(T)/dT] T \sim T_c$ . The gradient  $-d\mu_0 H_{c2}(T)/dT$  in the linear region near  $T_c$  is found to be about  $-1950$  mT/K. Consequently, the  $\mu_0 H_{c2}(0)$  value is found to be about 1130 mT. The Ginzburg-Landau (GL) coherence length at zero temperature  $\xi_{\text{GL}}(0)$  can be estimated to be  $171 \text{ \AA}$  by the relation  $\mu_0 H_{c2}(0) = \Phi_0 / 2\pi \xi_{\text{GL}}(0)^2$ .

The specific heat curves of  $C$  vs  $T$  below 300 K and  $C/T$  vs  $T^2$  at low temperatures are given in Figs. 5(a) and 5(b),

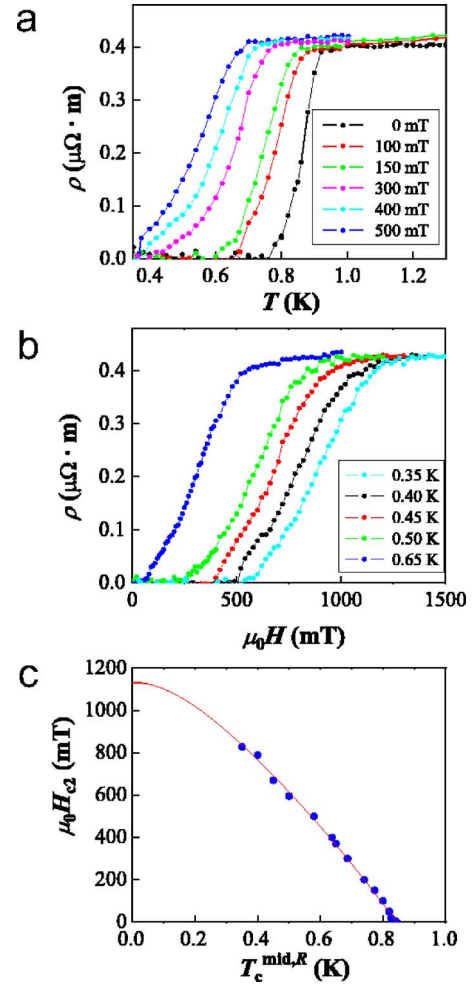


FIG. 4. (Color online) (a) Temperature dependence of the electrical resistivity ( $\rho$ ) under various magnetic fields. (b) Field dependence of the electrical resistivity ( $\rho$ ) at several temperatures. (c) Temperature dependence of the upper critical fields [ $\mu_0 H_{c2}(T)$ ] determined from the electrical resistivity data.

respectively. The  $C$ - $T$  curve shows the anomalies at the temperatures of the CDW ( $T_{\text{CDW}} \sim 250$  K) and superconducting transitions ( $T_c \sim 0.7$  K). A jump in the specific heat around 0.65 K is indicative of a bulk superconducting transition. The critical temperature from specific heat data is defined as the midpoint of the transition  $T_c^{\text{mid},C} = 0.66$  K. The specific heat in the normal state is composed of the electron and phonon contributions  $C = C_e + C_{\text{ph}}$ . Above  $T_c$  and much below the Debye temperature  $\Theta_D$ ,  $C/T$  is expressed by  $C(T)/T = (C_e + C_{\text{ph}})/T = \gamma + 12R\pi^4 T^2 / 5\Theta_D^3$ . From the  $C/T$ - $T^2$  plot in the normal metallic state, the values of  $\gamma$  and  $\Theta_D$  were obtained to be  $9.5 \text{ mJ/mol K}^2$  and  $194 \text{ K}$ , respectively. The electron-phonon coupling constant  $\lambda_{e\text{-ph}}$  is estimated from the McMillan equation for the superconducting transition temperature  $T_c = (\Theta_D / 1.45) \exp[-1.04(1 + \lambda_{e\text{-ph}}) / \lambda_{e\text{-ph}} - \mu^* (1 + 0.62\lambda_{e\text{-ph}})]$ , where the Coulomb pseudopotential  $\mu^*$  is assumed to be 0.13 empirically.<sup>9</sup> The value of  $\lambda_{e\text{-ph}}$  is determined to be 0.45. This small  $\lambda_{e\text{-ph}}$  value suggests that  $\text{Bi}_2\text{Rh}_3\text{Se}_2$  is classified into a weak-coupling superconductor.

The electronic specific heat  $C_e$  was obtained by subtract-

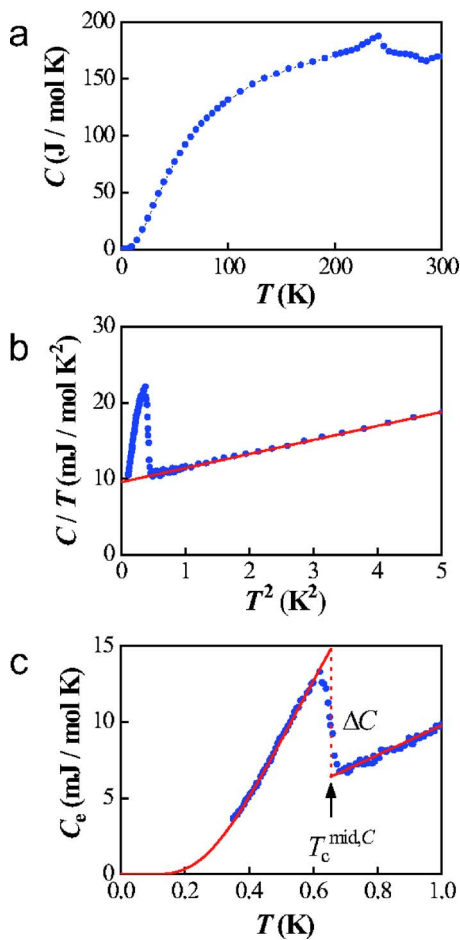


FIG. 5. (Color online) (a) Temperature dependence of the specific heat ( $C$ ) below 300 K. (b) Temperature dependence of the specific heat divided by temperature ( $C/T$ ) at low temperatures. (c) Temperature dependence of the electronic specific heat ( $C_e$ ) below 1 K.

ing  $C_{\text{ph}}$  from the total  $C$ , and the temperature dependence of  $C_e$  is plotted in Fig. 5(c). The specific heat jump  $\Delta C$  at  $T_c^{\text{mid},C}$

shows an evident energy gap in the superconducting state. Below  $T_c$ , the  $C$ - $T$  data follows the exponential decay. On the other hand, the fitting of a  $T^n$  function gives poor results. These fitting result shows that  $\text{Bi}_2\text{Rh}_3\text{Se}_2$  is an  $s$ -wave superconductor. The normalized specific heat jump value  $\Delta C/\gamma T_c^{\text{mid},C}$  is determined to be 1.35 and this value is slightly smaller than the limiting theoretical value ( $\Delta C/\gamma T_c^{\text{mid},C}=1.43$ ) of a weak-coupling superconductor. The result of the specific heat measurement reveals that  $\text{Bi}_2\text{Rh}_3\text{Se}_2$  is a typical BCS weak-coupling superconductor.

The thermodynamic critical field  $\mu_0 H_c(T)$  can be obtained as a function of temperature using the specific heat data in both normal the superconducting state. The difference in the entropy  $\Delta S(T)$  between the normal and superconducting states was obtained from the thermodynamic relation  $\Delta S(T)=S_n(T)-S_s(T)=\gamma T-\int_0^T[C_{es}(T')/T']dT'$ , where  $S_n(T)$  and  $S_s(T)$  are the entropies in the normal and superconducting states, respectively, and  $C_{es}$  is the electronic specific heat in the superconducting state. The  $C_{es}$  below 0.35 K is extrapolated by the exponential curve. The value of  $\mu_0 H_c(T)$  was obtained by the relation  $G_n(T)-G_s(T)=\int_T^{T_c}[\Delta S(T')/T']dT'=\mu_0 V_m H_c(T)^2/2$ , where  $V_m$  is the molar volume. The value of  $\mu_0 H_c(0)$  is calculated to be 5.31 mT. On the other hand, the BCS theory predicts the magnitude of  $\mu_0 H_c(T)$  by the relation  $\mu_0 H_c(T)=[0.47\mu_0\gamma T_c^2/V_m]^{1/2}$ . The value of  $\mu_0 H_c(0)$  is obtained to be 5.34 mT, which is close to the value of  $\mu_0 H_c(T)=5.31$  mT obtained from the thermodynamic relation.

Moreover, the penetration depth  $\lambda(0)$ , GL parameter  $\kappa(0)$  and lower critical field at zero temperature  $\mu_0 H_{c1}(0)$ , are estimated from the following relations:  $\mu_0 H_c(0)=\Phi_0/2\sqrt{2}\pi\lambda(0)\xi_{\text{GL}}(0)$ ,  $\kappa(0)=\lambda(0)/\xi_{\text{GL}}(0)$ ,  $\mu_0 H_{c1}=\mu_0 H_c \ln \kappa/\sqrt{2}\kappa$ . By using the value of  $\mu_0 H_c(0)=5.31$  mT,  $\lambda(0)$ , and  $\kappa(0)$ , and  $\mu_0 H_{c1}(0)$  are estimated to be 25700 Å and 151 and 0.12 mT, respectively. The considerably large value of  $\kappa(0)$  indicates that  $\text{Bi}_2\text{Rh}_3\text{Se}_2$  is an extreme type-II superconductor, like the high- $T_c$  cuprates, fullerenes<sup>10</sup> and cobalt oxyhydrate.<sup>11</sup>

\*Electronic mail: wake@sci.hokudai.ac.jp

<sup>1</sup>R. E. Peierls, *Quantum Theory of Solids* (Clarendon Press, Oxford, 1955).

<sup>2</sup>H. Flohlich, Proc. R. Soc. London, Ser. A **223**, 296 (1954).

<sup>3</sup>A. M. Gabovich and A. I. Voitenko, Low Temp. Phys. **26**, 305 (2000).

<sup>4</sup>A. M. Gabovich, A. I. Voitenko, J. F. Annett, and M. Ausloos, Semicond. Sci. Technol. **14**, R1 (2001).

<sup>5</sup>A. I. Baranov, A. V. Olenov, and B. A. Popovkin, Russ. Chem. Bull. **50**, 353 (2001).

<sup>6</sup>F. Izumi and T. Ikeda, Mater. Sci. Forum **321–324**, 198 (2000).

<sup>7</sup>G. Gruner, *Density Waves in Solids* (Addison-Wesley, Reading, MA, 1994).

<sup>8</sup>N. R. Werthamer, E. Helfand, and P. C. Hohenberg, Phys. Rev. **147**, 295 (1966).

<sup>9</sup>W. L. McMillan, Phys. Rev. **167**, 331 (1968).

<sup>10</sup>*Handbook of Superconductivity*, edited by C. P. Poole, Jr. (Academic Press, San Diego, 2000).

<sup>11</sup>G. Cao, C. Feng, Y. Xu, W. Lu, J. Shen, M. Fang, and Z. Xu, J. Phys.: Condens. Matter **15**, L519 (2003).